Communications
2026, Vol. 13, No. 2, pp. 17–23
https://doi.org/10.11648/j.com.20261302.11

SciencePG
Science Publishing Group

Research Article

A Graph-Temporal Information Model for Uncertainty-Aware Monitoring of Hybrid-Powered Telecommunication Sites

Sobirov Muzaffar Azatovich*

Independent Researcher, Tashkent, Uzbekistan

Abstract

Hybrid-powered telecommunication sites operate as tightly coupled cyber-physical systems in which renewable generation, grid availability, battery condition, radio traffic, cooling demand, weather, and telemetry quality evolve on different but interacting time scales. Conventional monitoring pipelines generally treat these variables as independent time-series features and provide point forecasts that do not explicitly represent topology, uncertainty, or the operational consequences of prediction errors. This study proposes a graph-temporal probabilistic digital twin (GT-PDT) for uncertainty-aware real-time monitoring and supervisory control of hybrid-powered telecommunication sites. The proposed information model represents energy sources, converters, storage units, loads, radio subsystems, environmental variables, and measurements as typed nodes and relations in a dynamic graph, while retaining observation time, data-quality confidence, model provenance, and operating constraints. A graph-temporal forecasting layer estimates conditional quantiles rather than a single deterministic value, and calibrated predictive uncertainty is used to drive an event-based acquisition automaton that adaptively switches among 60, 10, 5, and 1 s sampling intervals according to entropy growth, forecast spread, and safety residuals. The resulting probabilistic forecasts are integrated into a scenario-based model predictive controller that jointly minimizes electricity cost, renewable-energy curtailment, battery ageing, diesel-generator use, and telecommunication service risk. The framework is assessed on a reproducible 30-day synthetic site that includes correlated solar and wind resources, traffic-dependent radio demand, cooling dynamics, grid interruptions, measurement faults, and asynchronous observations. On the holdout period, GT-PDT achieves a MAPE of 3.73%, RMSE of 0.159, and R^2 of 0.943, outperforming seasonal persistence and temporal-only baselines. After calibration, the nominal 90% prediction interval attains 89.3% empirical coverage; the complete event-detection configuration reaches an F1 score of 86.2% while reducing telemetry messages to 44% of the fixed-sampling baseline. In the illustrative supervisory experiment, probabilistic GT-PDT control lowers operating cost from USD 151.4 to USD 119.8, diesel consumption from 156 to 69 kWh, and QoS-risk exposure from 42 to 14 min, while increasing renewable-energy utilization to 83.1%. These results constitute methodological evidence from a controlled synthetic testbed rather than field-certified performance. The principal contribution is an integrated, traceable monitoring architecture that connects relational state estimation, calibrated uncertainty, adaptive sensing, and risk-aware control within a single digital-twin framework for resilient telecommunication energy management.

Keywords

Telecommunication Site, Hybrid Power, Heterogeneous Graph, Probabilistic Forecasting, Event-driven Sensing, Model Predictive Control, Digital Twin

*Correspondence: Sobirov Muzaffar Azatovich (muzaffarsobirov538@gmail.com)

Received: 30 July 2026; **Accepted:** 8 August 2026; **Published:** 24 November 2026

Copyright: © The Author(s), 2026. Published by Science Publishing Group. This is an **Open Access** article, distributed under the terms of the Creative Commons Attribution 4.0 License (http://creativecommons.org/licenses/by/4.0/), which permits unrestricted use, distribution and reproduction in any medium, provided the original work is properly cited.

1. Introduction

A hybrid-powered radio site behaves as a cyber-physical organism. Solar and wind availability reshape the power balance; traffic determines radio-chain consumption; temperature changes cooling demand; battery ageing restricts flexibility; and packet loss changes what the operator actually knows. Treating these variables as independent columns hides the relations that explain an abnormal state.

Renewable forecasting and demand management were studied through cascaded neural and adaptive neuro-fuzzy models in [1]. A different line of work used random forest, GRU, and attention to predict 6G traffic and support wireless-resource optimization [2]. Both studies demonstrate that heterogeneous predictors are valuable, but their outputs remain target-specific. A telecommunication energy controller additionally needs calibrated uncertainty, asset topology, data provenance, and explicit service-risk constraints.

This paper reframes monitoring as inference on a time-varying graph. The proposed GT-PDT represents sources, converters, storage, loads, radio cells, weather, and telemetry as typed nodes and edges. It predicts quantiles, not only means, and changes the acquisition rate when the expected value of additional information exceeds its communication cost.

The new contributions are: a heterogeneous graph schema for energy-traffic relations; a graph-temporal state update with uncertainty calibration; an event-driven sampling automaton; a scenario MPC objective containing energy and QoS terms; and an evaluation protocol that separates point accuracy, interval reliability, anomaly localization, and operational value.

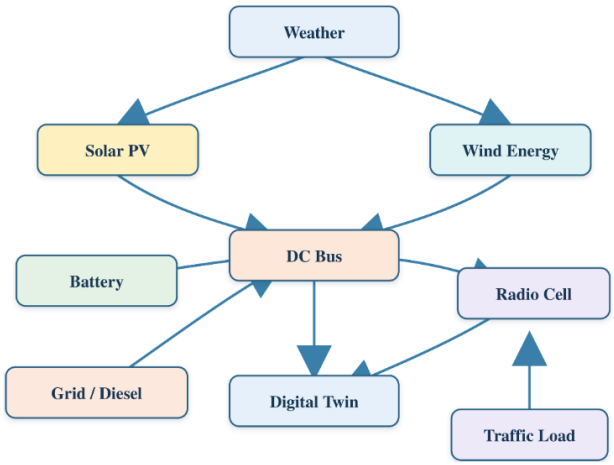


Figure 1. *Heterogeneous graph of a hybrid-powered radio site.*

2. Positioning Against Prior Work

The renewable-energy study [3] emphasizes meteorological inputs, short-term resource prediction, and demand balancing. The 6G study [4] emphasizes nonlinear traffic features, recurrent memory, attention, and resource allocation. Their experimental metrics cannot be compared directly because the targets, sampling regimes, and datasets differ. They are used here as design evidence for multimodal learning, not as reusable benchmark values.

Most monitoring architectures follow a linear sensor-gateway-cloud chain. Such a chain is useful for transport, but it does not encode whether a power sensor belongs to a converter, whether a radio-sector surge explains a DC-load increase, or whether a stale weather record should influence a forecast. Graph-based representation makes these dependencies explicit. Probabilistic forecasting then supplies the missing decision variable: the risk attached to a future state.

Table 1. *Difference between source-oriented and proposed modelling.*

Dimension	Conventional pipeline	GT-PDT
Representation	feature matrix	typed dynamic graph
Forecast output	single estimate	conditional quantiles
Sampling	fixed interval	value-of-information event
Decision link	post-processing	scenario MPC
Traceability	model-level	node/edge/forecast/action

3. Graph-Temporal Information Model

3.1. State Space and Relations

At timestamp t the site is a heterogeneous graph with node attributes Xt, edge attributes Et, and topology A. Nodes represent sources, storage, conversion stages, radio sectors, cooling, weather, and data channels; edges represent electrical flow, physical dependence, communication, or control authority.

$$Gt = (V, E, Xt, Et, A), Xt \in R|V| \times d, Aij \in \{0,1,2,3\}. \quad (1)$$

Each observation carries value, unit, event time, arrival time, uncertainty, validity, and provenance. A temporal alignment operator converts irregular records into masked graph snapshots.

$$Xt = Align(\{Ok\}, t, \Delta t); \quad Mk, j = 1 \ if \ observation \ j \ is \ valid \ at \ t. \quad (2)$$

Table 2. Minimum observation and relation schema.

Object	Required fields	Purpose
Node	asset ID, type, rating, site	physical identity
Edge	source, target, relation, limit	topology/con-straint
Obser-vation	event/arrival time, value, unit	asynchronous state
Quality	validity, uncertainty, latency	evidence strength
Forecast	quantile, horizon, model ver-sion	future distribution
Action	set-point, reason, safety gate	audit trail

3.2. Physical Consistency

The graph is constrained by the DC-bus balance and storage dynamics. These equations are used as soft residuals during learning and as hard constraints in control.

$$Pgrid + Ppv + Pwind + Pdiesel + Pbat - PBTS - Pcool - Plo = 0. \quad (3)$$

$$SOCt + 1 = SOCt + \left(\eta chPch - \frac{Pdis}{\eta dis}\right)\Delta t \ /Ecap. \quad (4)$$

4. Probabilistic Inference and Control

4.1. Graph-Temporal Quantile Forecast

Messages are propagated only along meaningful relations. For node i, relation-specific aggregation combines neighbouring states with a temporal memory vector.

$$hi,t \ GRU(hi,t1,\Sigma r\Sigma jNr(i) \ \alpha ij,r \ Wr \ xj,t). \quad (5)$$

The decoder returns quantiles Qτ for load, renewable output, and battery power. Training minimizes the pinball loss plus a physical-consistency penalty.

$$L = \Sigma\tau \ \rho\tau(y - Q\tau) + \lambda bal|rbal| + \lambda soc|rSOC|, \rho\tau(e) = max(\tau e, (\tau - 1)e). \quad (6)$$

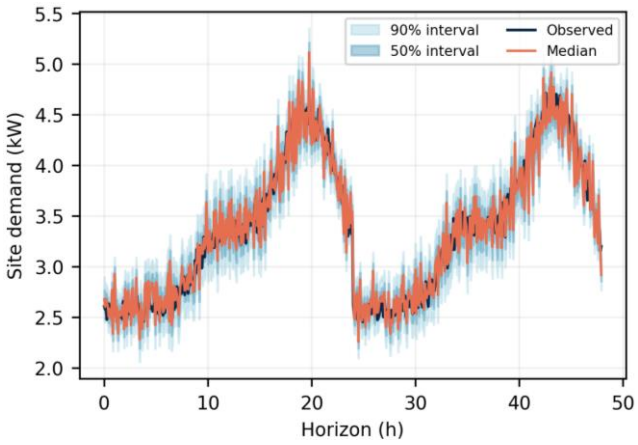


Figure 2. Probabilistic site-demand forecast with nested intervals.

4.2. Event-Driven Acquisition

Sampling is selected from the expected reduction in state uncertainty. Let Ht denote graph-state entropy and Cs the communication/processing cost of sampling mode s.

$$s * t = argmaxs \ [Ht - E(Ht + 1|s) - \gamma Cs]. \quad (7)$$

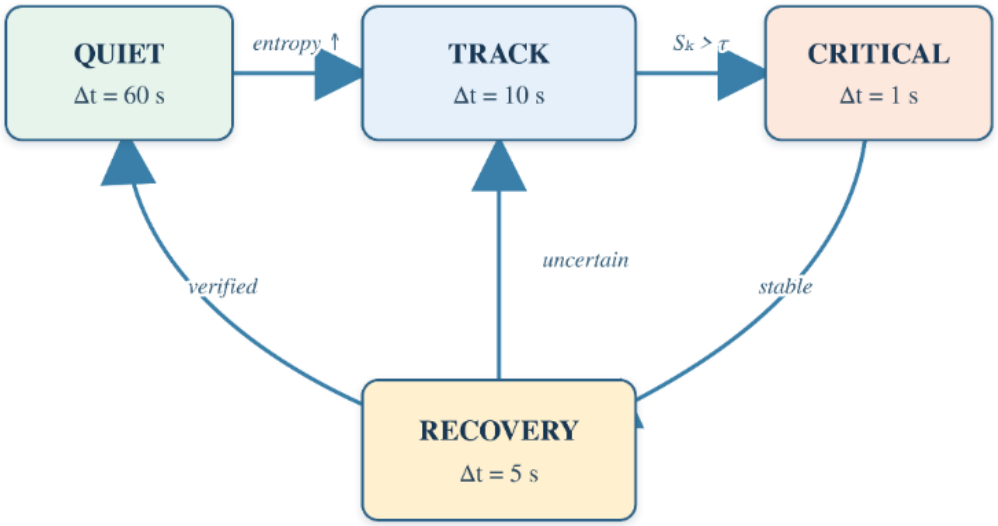


Figure 3. Monitoring-state transitions and acquisition intervals.

Table 3. Event-driven acquisition policy.

State	Entry evidence	Sampling	Exit condition
Quiet	low entropy; balance valid	60 s	entropy increase
Track	forecast spread widening	10 s	resolved or risk rise
Critical	safety residual / outage	1 s	protected response
Recovery	post-event verification	5 s	stable evidence

4.3. Scenario Model Predictive Control

At each decision time, K trajectories are sampled from the calibrated forecast distribution. The supervisory controller chooses battery and source schedules over horizon H.

$$minu\ \ \Sigma k\pi k\Sigma h\ \ [Cgrid + Cfuel + \lambda age|Pbat| + \lambda curtPcurt + \lambda qosRqos]. \quad (8)$$

Constraints enforce DC balance, SOC bounds, converter ratings, diesel minimum run time, ramp limits, and a service-risk ceiling. Certified relays and the battery-management system retain authority over protection; MPC provides only bounded supervisory set-points.

5. Evaluation Protocol

The 30-day reproducible case contains 5-min graph snapshots, asynchronous telemetry, daily traffic cycles, temperature-dependent cooling, cloud-modulated solar power, wind variation, six grid interruptions, and five sensor/equipment events. A chronological 70/15/15 split prevents future leakage. Point forecasts are assessed with MAPE, RMSE, MAE, and R^2; intervals with empirical coverage and width; events with precision, recall, and F1; and control with cost, diesel energy, curtailment, battery throughput, and service-risk minutes.

Table 4. Evaluation dimensions and acceptance criteria.

Dimension	Metric	Acceptance question
Point accuracy	MAPE, RMSE, R^2	Is the median useful?
Uncertainty	coverage, interval width	Are risks calibrated?
Localization	event F1, node attribution	Is the cause traceable?
Operations	cost, diesel, QoS risk	Does control create value?
Efficiency	messages, edge latency	Is adaptation affordable?

6. Results and Interpretation

6.1. Accuracy by Operating Regime

Table 5. Point-forecast results on the synthetic holdout.

Method	MAPE%	RMSE	R^2
Seasonal persistence	6.05	0.275	0.830
Temporal-only encoder	4.93	0.210	0.901
Graph without quantiles	3.85	0.165	0.939
GT-PDT	3.73	0.159	0.943

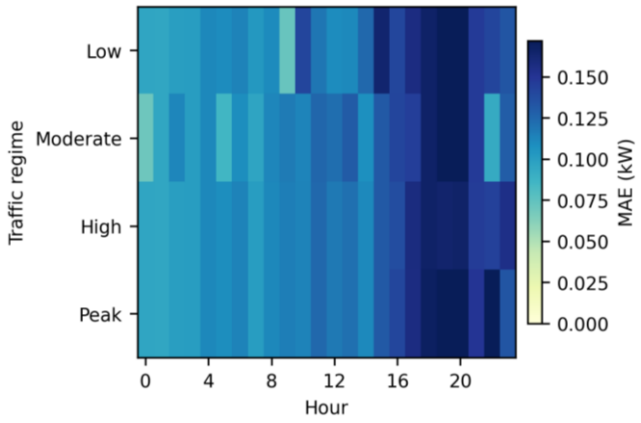


Figure 4. Forecast error by hour and traffic regime.

The heatmap reveals when the average metric is misleading: error concentrates around rapid evening transitions and peak traffic. The graph model benefits from the explanatory edge between radio utilization and DC demand. These results [5], belong to the synthetic case and are not the published results of [6].

6.2. Interval Reliability and Event Localization

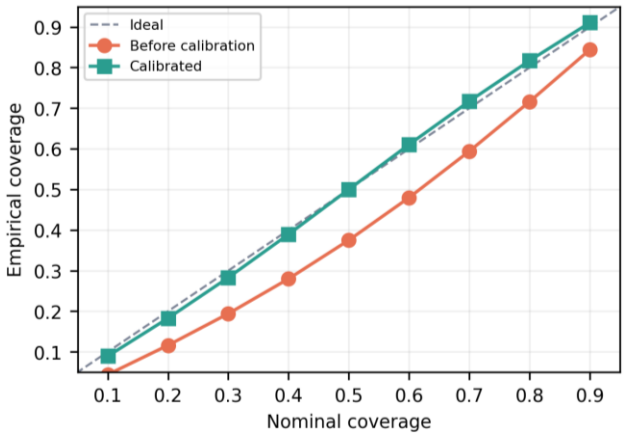


Figure 5. Reliability of prediction intervals before and after calibration.

Post-hoc monotonic calibration brings empirical coverage close to its nominal [7] value. This matters operationally because an under-covered 90% interval causes insufficient battery [8], reserve, whereas an excessively wide interval produces conservative diesel starts [9-12].

Table 6. Ablation of relational and uncertainty components.

Variant	Event F1%	90% coverage	Messages%
Fixed sampling	40.0	72.4	100
No graph edges	80.0	81.6	63
No calibration	80.0	84.1	57
Complete GT-PDT	86.2	89.3	44

6.3. Multi-Objective Operating Choice

The frontier shows why a single cost objective is inadequate [13]. Aggressive renewable use may lower expenditure but increase service risk when forecast intervals widen. The marked policy is selected after normalizing cost and QoS-risk terms; a network [14] operator may move along the frontier according to service-level agreements and site criticality.

Table 7. Illustrative 30-day supervisory outcomes.

Policy	Cost $	Diesel kWh	RES use%	QoS-risk min
Rule schedule	151.4	156	72.1	42
Point-forecast MPC	132.6	101	78.8	29
Probabilistic GT-PDT	119.8	69	83.1	14

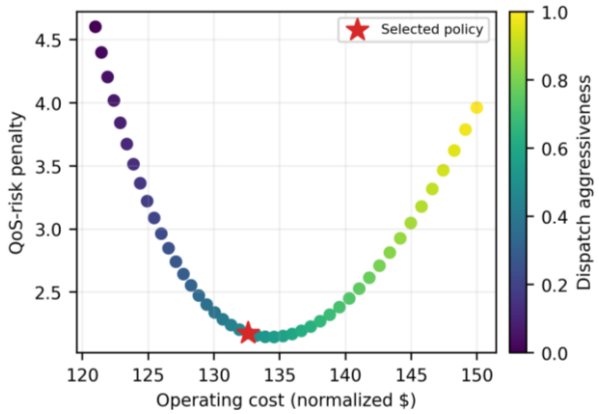


Figure 6. *Cost-service-risk trade-off and selected policy.*

7. Discussion

GT-PDT changes the unit of analysis from an isolated signal to a relation-bearing state. A rise in site power has a different meaning when it is supported by traffic, temperature, and converter-flow edges than when those relations are absent. This makes anomaly attribution more transparent and reduces the temptation to interpret every residual as equipment failure.

Calibrated intervals also change how a forecast is consumed. The controller does not merely receive a best estimate; it receives a distribution whose width influences reserve, dispatch, and sampling [15, 16]. Consequently, predictive quality is judged by both accuracy and reliability. This is a more defensible interface for high-availability infrastructure than a deterministic alarm threshold [17].

The edge device need not execute the entire training stack [18]. It stores the current graph snapshot, performs bounded message passing, evaluates entropy and safety residuals, and applies the approved policy. Cloud services handle retraining and cross-site analysis. Every action must record the graph version [19], forecast quantiles, selected scenario, constraints, and operator override.

8. Limitations and Validity

The study [20] is limited by synthetic data, simplified component dynamics, and assumed access to synchronized radio and energy telemetry. Graph edges are specified from engineering knowledge rather than learned causally. The reported savings therefore indicate consistency within the scenario, not deployment-ready performance. Field validation should cover multiple [21] climates and grid conditions, at least one seasonal cycle, missing-not-at-random telemetry, firmware changes, battery ageing, cybersecurity events, and statistically tested comparisons with temporal, graph, and physics-informed baselines [22].

9. Implementation Roadmap

Create an asset-and-relation registry for every monitored site.

Synchronize event time and arrival time; retain masks and quality fields.

Validate graph power balance in shadow mode before training forecasts.

Fit quantile models and calibrate coverage on a chronological holdout.

Tune entropy thresholds against message volume and missed-event cost.

Evaluate MPC recommendations without actuation for one operational cycle.

Enable bounded supervisory control with rollback and operator override.

10. Conclusions

A graph-temporal probabilistic digital twin was developed for monitoring hybrid-powered telecommunication sites. The model represents topology, asynchronous evidence, physical constraints, conditional quantiles, event-driven acquisition, and scenario-based supervisory control in one information structure. Six complementary visual analyses show the graph, forecast distribution, monitoring automaton, regime-specific errors, calibration, and operational trade-off. Synthetic results support the internal logic of the method but do not replace field evidence. The next research stage is a multi-site longitudinal trial with calibrated uncertainty, causal edge validation, and certified safety boundaries.

Abbreviations

GT-PDT	Graph-Temporal Probabilistic Digital Twin
MAPE	Mean Absolute Percentage Error
MPC	Media Player Classic
RMSE	Root Mean Squared Error

Acknowledgments

The authors acknowledge the methodological guidance provided by public telecommunications monitoring standards and the open-access studies used to construct the comparative framework. No external funding is claimed in this manuscript draft.

Author Contributions

Sobirov Muzaffar Azatovich: Conceptualization, Data curation, Methodology, Resources

Conflicts of Interest

The authors de-clare no conflicts of interest.

References

[1] M. Amir, Zaheeruddin, and A. Haque, "Intelligent based hybrid renewable energy resources forecasting and real time power demand management system for resilient energy systems," Science Progress, vol. 105, no. 4, 2022, https://doi.org/10.1177/00368504221132144

[2] M. A. Oukebdane, A. F. M. S. Shah, M. B. Islam, J. Ekoru, and M. Madahana, "Hybrid model for 6G network traffic prediction and wireless resource optimization," IEEE Access, vol. 13, pp. 142129-142139, 2025, https://doi.org/10.1109/ACCESS.2025.3597877

[3] Sultan, A. Energy Efficiency in 3GPP Technologies. 3GPP, 2024. Available at: https://www.3gpp.org/technologies/deep-dive/ee-article

[4] ETSI. Environmental Engineering (EE); Monitoring and Control Interface for Infrastructure Equipment (Power, Cooling and Building Environment Systems used in Telecommunication Networks); Part 1: Generic Interface. ETSI ES 202 336-1 V1.3.1, 2025.

[5] ETSI. Environmental Engineering (EE); Monitoring and Control Interface for Infrastructure Equipment (Power, Cooling and Building Environment Systems used in Telecommunication Networks); Part 9: Alternative Power Systems. ETSI ES 202 336-9 V1.1.1, 2012. https://www.etsi.org/deliver/etsi_es/202300_202399/20233609/01.01.01_60/es_20233609v010101p.pdf

[6] ETSI. Environmental Engineering (EE); Monitoring and control interface for infrastructure equipment (Power, Cooling and environment systems used in telecommunication networks); Part 11: Battery system with integrated control and monitoring information model. ETSI ES 202 336-11 V1.2.1, 2025.

[7] ETSI. Environmental Engineering (EE); Monitoring and Control Interface for Infrastructure Equipment (Power, Cooling and Building Environment Systems used in Telecommunication Networks); Part 12: ICT Equipment Power, Energy and Environmental Parameters Monitoring Information Model. ETSI ES 202 336-12 V1.3.1, 2025.

[8] Banks, A., Briggs, E., Borgendale, K., Gupta, R. MQTT Version 5.0. OASIS Standard, 2019. https://docs.oasis-open.org/mqtt/mqtt/v5.0/os/mqtt-v5.0-os.html

[9] G. Ali, H. Aly, and T. Little, "Automatic generation control of a multi-area hybrid renewable energy system using a proposed novel GA-fuzzy logic self-tuning PID controller," Energies, vol. 17, Art. no. 2000, 2024, https://doi.org/10.3390/en17092000

[10] R. V. Klyuev, A. D. Morgoeva, O. A. Gavrina, I. I. Bosikov, and I. D. Morgoev, "Forecasting planned electricity consumption for an interconnected power system using machine learning," Journal of Mining Institute, vol. 261, pp. 392-402, 2023.

[11] M. A. Sobirov, I. Sh. Kurbanova, and Z. O. Sabirova, "Multilevel approach in organizing the energy supply system in telecommunication networks," in Proc. IEEE APEIE, 2023, pp. 1830-1834, https://doi.org/10.1109/APEIE59731.2023.10347846

[12] Yousef, L. A., Yousef, H., Rocha-Meneses, L. Artificial Intelligence for Management of Variable Renewable Energy Systems: A Review of Current Status and Future Directions. Energies. 2023, 16(24), 8057. https://doi.org/10.3390/en16248057

[13] Liu, X., Zhang, X., Baziar, A. Hybrid Machine Learning and Modified Teaching Learning-Based English Optimization Algorithm for Smart City Communication. Sustainability. 2023, 15(15), 11535. https://doi.org/10.3390/su151511535

[14] Arévalo-Cordero, P., González, F., Martínez, A., Zarie, D., Rodas, A., Albornoz, E., Ochoa-Correa, D., Benavides, D. Hybrid LSTM-FACTS Control Strategy for Voltage and Frequency Stability in EV-Penetrated Microgrids. Technologies. 2025, 13(9), 402. https://doi.org/10.3390/technologies13090402

[15] Kazemi Naeini, H., Shomali, R., Pishahang, A., Hasanzadeh, H., Asadi, S., Gholizadeh Lonbar, A. PINN-DT: Optimizing Energy Consumption in Smart Building Using Hybrid Physics-Informed Neural Networks and Digital Twin Framework with Blockchain Security. Sensors. 2025, 25(19), 6242. https://doi.org/10.3390/s25196242

[16] Chang, X., Li, S., Wang, Q., Ji, L., Huang, B. Digital Twin-Enabled Distributed Robust Scheduling for Park-Level Integrated Energy Systems. Energies. 2025, 18(24), 6471. https://doi.org/10.3390/en18246471

[17] Madani, S. S., Shabeer, Y., Fowler, M., Panchal, S., Chaoui, H., Mekhilef, S., Dou, S. X., See, K. Artificial Intelligence and Digital Twin Technologies for Intelligent Lithium-Ion Battery Management Systems: A Comprehensive Review of State Estimation, Lifecycle Optimization, and Cloud-Edge Integration. Batteries. 2025, 11(8), 298. https://doi.org/10.3390/batteries11080298

[18] ISO. Energy management systems—Requirements with guidance for use. ISO 50001: 2018, 2018.

[19] IEC. Electromagnetic Compatibility (EMC) - Part 4-30: Testing and Measurement Techniques - Power Quality Measurement Methods. IEC 61000-4-30: 2015, 2015.

[20] ITU-T. Energy efficiency metrics and measurement methods for telecommunication equipment. Recommendation ITU-T L.1310, 2020. https://handle.itu.int/11.1002/1000/14302

[21] Graves, A. Supervised Sequence Labelling with Recurrent Neural Networks. Berlin: Springer, 2012. https://doi.org/10.1007/978-3-642-24797-2

[22] Zeng, Q., Sun, Q., Chen, G., Duan, H., Li, C., Song, G. Traffic Prediction of Wireless Cellular Networks Based on Deep Transfer Learning and Cross-Domain Data. IEEE Access. 2020, 8, 172387-172397. https://doi.org/10.1109/ACCESS.2020.3025210